Hindawi
Advances in Civil Engineering
Volume 2022, Article ID 8931401, 10 pages
https://doi.org/10.1155/2022/8931401

Research Article

Shrinkage and Mechanical Properties of Fibre-Reinforced Blast Furnace Slag-Steel Slag-Based Geopolymer

Shengtang Xu,[1,2] **Chaofan Wu**,[3] **Jinchao Yue**,[1] **and Zikai Xu**[1,4]

[1]*School of Water Conservancy Engineering, Zhengzhou University, Zhengzhou 450001, Henan, China*
[2]*Xinyang Highway Development Center, Xinyang 464000, Henan, China*
[3]*Xi'an Changda Highway Maintenance Technology Co. Ltd, Xi'an 710000, Shanxi, China*
[4]*College of Highway, Chang'an University, Xi'an, 710064, Shanxi, China*

Correspondence should be addressed to Zikai Xu; xuzikai@chd.edu.cn

Received 13 December 2021; Accepted 21 March 2022; Published 8 April 2022

Academic Editor: Md. Akter Hosen

Geopolymer materials have several obvious advantages such as energy conservation, emission reduction, and waste reuse, so they can become substitutes for cement materials. In this study, geopolymer mortars made from blast furnace slag and steel slag reinforced by basalt fibre and polyvinyl alcohol (PVA) fibre were prepared to explore the effect on their strength and shrinkage properties. Scanning electron microscopy (SEM) was employed to characterize the reaction mechanism of the geopolymer mortars. The results show that both PVA fibre and basalt fibre can improve the mechanical properties of geopolymer mortars during the late curing period. The geopolymer reinforced by basalt fibre manifested a better toughness. A proper content of PVA fibres and basalt fibres can effectively reduce the drying and autogenous shrinkage of geopolymer mortars. The optimal content of basalt fibres and PVA fibres to reduce the drying shrinkage was 0.4%. The SEM results show that the fibres can effectively alleviate the stress concentration and prevent crack propagation.

1. Introduction

In recent years, cement mortar has been widely used in concrete repair and reinforcement materials due to its advantages of low cost, convenient construction, and stable properties. However, the large-scale use of cement has produced increasingly serious problems such as energy consumption, resource consumption, and environmental pollution. Geopolymers are a new type of nonmetallic material prepared from natural Si-Al-containing materials or industrial slags such as slag, fly ash, and steel slag [1–3]. Geopolymers exhibit excellent characteristics including high strength, low CO_2 emissions, excellent corrosion resistance, and durability compared to traditional cementitious binders [4–6].

Therefore, many researchers have used geopolymer materials to prepare mortars and made great efforts to improve their properties. Helmy [7] suggested that intermittent curing proved an increase in compressive strength of all geopolymer mortars prepared by fly ash at the end of each curing step. Atis et al. [8] believed that an increase in heat curing temperature and heat curing durations was beneficial to enhance the compressive strength of geopolymers. Fly-ash-based geopolymer pastes reached 120 MPa when activated with 14% NaOH and cured at 115°C for 24 h. Ilkentapar et al. [9] found that the water absorption of fly ash-based geopolymer mortars increased with increasing heat curing duration. An extra rest period of curing after heat curing increases the water absorption. Yang et al. [10] found that the substitution of fly ash decreased the reactivity of the solid precursors of metakaolin-based geopolymer mortars, which resulted in a lower reaction rate, a longer reaction time, and an obstruction of water evaporation from pore networks. Elyamany et al. [11] explored the effect of sodium hydroxide molarity on the setting time of geopolymer mortars. Some results showed that the setting time decreased with increasing NaOH solution molarity possibly because increasing the NaOH molarity can improve the dissolution

rate of the aluminosilicate precursors and enhance the geopolymerization process. Chen et al. [12] revealed that when the replacement ratio of GGBS reached 30%, the mortar had better compressive strength (75.9 MPa), flexural strength (12.2 MPa), and bond strength (6.4 MPa) than many pavement repair materials.

However, geopolymer mortars have disadvantages of high brittleness, low toughness, and low deformation resistance, which is similar to cement mortars. However, the addition of various fibres can significantly improve these properties. For example, Zhang et al. [13] experimentally concluded that the compressive strength and fracture energy of geopolymer mortars could be improved by mixing a certain amount of PVA fibre. Malik [14] suggested that the structural properties and durability of geopolymers were improved by incorporating 5% PVA fibres. Microstructural studies confirmed that PVA fibres in geopolymer matrices were well distributed to develop a fibre-bridging texture with improved performance. Guo [15] found that basalt fibres could also significantly improve the 28-d compressive and flexural strength of geopolymer mortars and effectively prevent cracking and crack propagation, as shown in scanning electron micrographs. Punurai [16] found that basalt fibre could make geopolymer pastes more uniform and denser with a smaller total porosity. Therefore, PVA fibres or basalt fibres can be used to enhance the toughness and durability of geopolymer mortars.

The obvious shrinkage during the setting and hardening processes is another important factor that affects the wide-area applications of geopolymers [17, 18]. Excessive shrinkage will result in cracking, which further reduces the strength, stiffness, and service life of the structure [10, 19, 20]. Much effort has been made by scholars to study the shrinkage properties of geopolymers. Studies have shown that an increase in the addition of fly ash can significantly reduce the drying shrinkage of geopolymers due to the microaggregate filling effect of fly ash [21, 22]. In addition, the NaOH concentration has a serious effect on the drying shrinkage of geopolymers. The geopolymers prepared by a higher NaOH molarity showed a lower drying shrinkage and a higher autogenous shrinkage [23]. Ridtirud et al. [24] found that the curing temperature and solid/liquid ratio played key roles in determining the drying shrinkage of fly-ash-based geopolymers. Duan et al. [25] believed that the incorporation of TiO_2 nanoparticles into geopolymers could improve the carbonation resistance of geopolymers and reduce drying shrinkage.

In this article, steel slag and slag are used as raw materials to prepare geopolymer mortar. Steel slag and slag can promote each other under the action of an alkaline exciter due to the difference in activity. Due to the rapid reaction in the early stage and lack of Ca^{2+} in the later stage, while the steel slag has a high CaO content, $Ca(OH)_2$ generated by the reaction can be absorbed by the slag to promote the hydration of the slag. The absorption of Ca^{2+} by the slag promotes the dissociation hydration of the steel slag and generates products such as hydrated calcium aluminosilicate and zeolite to fill the pores, which form in the early stage of the reaction. In addition, mixing the fibre material is expected to improve the toughness and reduce the shrinkage of the geopolymer. Thus, further research on restricting the shrinkage of geopolymer mortars by adding PVA fibre or basalt fibre is meaningful, but relevant research remains insufficient. Geopolymers made from slag and steel slag with various mixed volume ratios of PVA fibres and basalt fibres are prepared to explore the effect on the shrinkage and mechanical properties of geopolymer mortars.

2. Experimental

2.1. Materials. Blast furnace slag and steel slag were used as the raw materials to prepare geopolymer binders, and quartz sand with a particle size of 40–70 mm was used as the fine aggregate. The specific surface area of the blast furnace slag powder is 436 m^2/kg. The blast furnace slag mainly consisted of 37.2% CaO, 30.0% SiO_2, and 16.6% Al_2O_3, as shown in Table 1. Steel slag is a type of solid waste discharged from steelmaking, and its chemical composition is affected by factors such as the iron ore source, slagging material, and steelmaking methods. The chemical composition of steel slag in this study is mainly composed of 30.1% CaO, 15.3% SiO_2, 33.2% Fe_2O_3, and 15.0% MgO, as shown in Table 1, with a specific surface area of 420 m^2/kg.

The chosen modulus of the sodium silicate solution ($M = n$ (SiO_2)/n (Na_2O)) was 3.2, which was adjusted by NaOH and used as a composite alkali activator. The modulus of the composite alkali activator was 1.2. The solid contents of Na_2O and SiO_2 were 8.5% and 26.8%, respectively.

Polyvinyl alcohol fibres (PVA fibres) 12 mm in length and 15 μm in diameter and basalt fibres (BF) 12 mm in length and 13 μm in diameter were used. Their technical indicators are shown in Table 2.

2.2. Mix Proportions of Geopolymer Mortars. Table 3 presents the mix proportions of the geopolymer mortars. The ratio of water to binder was 0.55 (including the water in activator), the ratio of binder to sand was 0.60, and the equivalent of Na_2SiO_3 in activator to the binder material was 22%. The addition of 0.1%, 0.2%, 0.3%, and 0.4% PVA fibres (PVA-1, PVA-2, PVA-3, and PVA-4, respectively) was selected for comparison with the control sample (PVA-0), and all proportions were expressed in volume ratio (%). Samples mixed with a 0.1–0.4% volume ratio of basalt fibres (named BF-1, BF-2, BF-3, and BF-4) were also prepared.

2.3. Preparation of Geopolymer Mortars. The geopolymer mortars had a similar preparation process to cement pastes. First, the fibres were put into activators and mixed to be well distributed, and the mixture was poured into a cement mortar mixer with water, blast furnace slag, steel slag, and quartz sand. Then, the mixture was stirred for 120 s at low speed in the mixer prior. After 180 s of stirring at high speed, the geopolymer mortars were poured into moulds with dimensions of 70.7 × 70.7 × 70.7 mm and 40 × 40 × 160 mm.

Table 1: Chemical composition of blast furnace slag and steel slag.

Materials	Chemical composition (wt%)					
	CaO	SiO_2	Al_2O_3	MgO	SO_3	Fe_2O_3
Blast furnace slag	37.20	30.03	16.58	9.17	3.92	0.76
Steel slag	30.12	15.32	3.80	15.00	1.09	33.24

Table 2: Technical indexes of PVA and basalt fibre.

Type	Length (mm)	Diameter (μm)	Tensile modulus (MPa)	Initial modulus (GPa)	Density (g/cm^3)
PVA fibre	12	15	1830	40	1.29
Basalt fibre	12	13	4500	101	2.64

Table 3: Mix proportions of geopolymer mortars.

Samples	Slag (%)	Steel slag (%)	Activator modulus	Activator concentration (%)	Water binder ratio	Binder sand ratio	Fibre content (%)
PVA-0	70	30	1.2	22	0.50	0.60	0
PVA-1	70	30	1.2	22	0.50	0.60	0.1
PVA-2	70	30	1.2	22	0.50	0.60	0.2
PVA-3	70	30	1.2	22	0.50	0.60	0.3
PVA-4	70	30	1.2	22	0.50	0.60	0.4
BF-1	70	30	1.2	22	0.50	0.60	0.1
BF-2	70	30	1.2	22	0.50	0.60	0.2
BF-3	70	30	1.2	22	0.50	0.60	0.3
BF-4	70	30	1.2	22	0.50	0.60	0.4

2.4. Testing Methods

2.4.1. Mechanical Properties. According to the standard of cement test methods to determine the strength (ISO 679 : 2009), the compressive strength ($70.7 \times 70.7 \times 70.7$ mm) and flexural strength (40 mm × 40 mm×160 mm) of the specimens were tested at curing ages of 3 d, 7 d, and 28 d in a microcomputer-controlled pressure testing system. The samples were cured in a standard curing box (20°C and >95% RH) until the specified age was reached. The compressive strength and flexural strength were the averages of six separate tests. Data deviating by more than 10% of the mean were eliminated.

Figure 1: Comparator and dial indicators.

2.4.2. Drying Shrinkage. According to the standard test method (JC/T 603–2004), the drying shrinkage was reported by measuring three specimens to obtain an average value. After demoulding, the samples were further cured in a 20°C water bath for 2 days and subsequently removed. The water on the surface of the specimens was wiped, and the initial length was measured with an accuracy of 0.001 mm, as shown in Figure 1. Afterwards, the samples were put into a drying and shrinking box to cure at a temperature of 20 ± 2°C and a relative humidity of 60 ± 5%. The length of the samples after curing was tested with an accuracy of 0.001 mm. Drying shrinkage is determined as follows:

$$\varepsilon = \frac{L0 - L\,d}{160} \times 100\%, \quad (1)$$

where ε is the drying shrinkage, L_0 (mm) is the demoulded length, L_d (mm) is the measured length, and 160 (mm) is the effective length of the specimens without two head nails.

2.4.3. Autogenous Shrinkage. The autogenous shrinkage test was performed using a beam specimen with a size of $40 \times 40 \times 160$ mm. After 24 h of moulding, the specimens were removed from the mould, immediately sealed with polyethylene film, and wrapped with a layer of self-adhesive tin foil. Autogenous shrinkage is determined as follows:

$$\sigma = \frac{L1 - Lt}{160} \times 100\%. \quad (2)$$

The initial length L1 was measured with a length-ratio metre, and Lt was measured after setting to the specified age.

2.4.4. Mass Loss. The mass loss rate was used to measure the mass change under identical curing conditions to the drying shrinkage test. The mass loss is determined as follows:

$$\Delta m = \frac{Ws - Wt}{Ws}. \quad (3)$$

Here, Δm(wt%) is the mass loss, Ws is the initial weight of the specimens, and Wt is the measurement weight of the specimens at t days.

3. Results and Discussion

3.1. Compressive and Flexural Strength of Basalt Fibre-Reinforced Geopolymer Mortars. The compressive strengths of geopolymer mortars with different basalt fibre contents after 3 d, 7 d, and 28 d of curing are shown in Figure 2(a). The compressive strength of the samples at 3 d and 7 d slightly decreased after basalt fibres was added. The compressive strength was higher than that of the control group only when the fibre content was 0.3%. After 28 d of curing, the compressive strength first increased and subsequently decreased with the increase in the fibre content, and all strengths were higher than that of the control group. The compressive strength of the mortars reached a maximum of 41.1 MPa when 0.2% fibre was added, which is 11.7% higher than that of the control group.

Figure 2(b) shows the flexural strength of geopolymer mortars with different basalt fibre contents at curing ages of 3 d, 7 d, and 28 d. The flexural strength of geopolymer mortars increased when the basalt fibre content increased from 0.1% to 0.3%. When the basalt fibre content further increased, the flexural strength slightly decreased, and the compressive strength remained higher than that of the control group. The optimal content of basalt fibre is approximately 0.2%, and the early flexural strength reached a maximum of 5.4 MPa and 6.1 MPa for 3 d and 7 d of curing. If the content of basalt fibre was 0.3%, the flexural strength at 28 d of curing age reached the maximum of 7.4 MPa and increased by 17.4% compared to the control sample. The optimal basalt fibre content for compressive strength development is 0.2-0.3%.

The basalt fibre can be uniformly dispersed in specimens to form a mesh structure, which effectively resists crack extension and enhances the structural toughness [26]. Adding a proper content of fibres is beneficial to energy absorption and strength development. However, too many fibres are difficult to mix well in mortars, which results in an uneven structure with excessive porosity defects [27].

3.2. Compressive and Flexural Strength of PVA Fibre-Reinforced Geopolymer Mortars. The compressive strength of geopolymer mortars at 3 d, 7 d, and 28 d of curing with different PVA fibre contents is shown in Figure 3(a). The incorporation of PVA fibres reduced the compressive strength of mortars at 3 d of curing except when 0.2% of PVA fibres was added. The 7-d compressive strength appeared to decrease with the increasing incorporation of PVA fibres. If the content of PAV fibres was less than 0.2%, the compressive strength at 28 d of curing age obviously improved. However, if the content was higher than 0.2%, the compressive strength at 28 d of curing decreased. This strength was even lower than that of the control group, while the content was 0.4%. The highest 28-d compressive strength of geopolymer mortars (prepared with 0.2% content of PVA fibres) was 41.8 MPa, which is 13.6% higher than that of the control sample.

Figure 3(b) shows the flexural strength of geopolymer mortars with different PVA fibre contents at 3 d, 7 d, and 28 d of curing ages. The results show that the 3-d flexural strength reached a maximum value of 4.3 MPa at a PVA fibre content of 0.2%. The 7-d flexural strength at various PVA fibre contents was slightly higher than that of the control group. The reinforcing effect of PVA fibres on geopolymer mortars was obvious at 28 d of curing. The optimal content of PVA fibres for 28 d flexural strength gain was 0.2%, and the corresponding strength reached 7.6 MPa, which is 20.6% higher than that of the control sample. Similar to the trends of the compressive strength, an excessive content (>0.2%) is expected to weaken the reinforcing effect of PVA fibres.

The PVA fibre significantly contributed to the compressive and flexural strength gain at the later curing age (28 d), which is consistent with the report in [15]. The optimal PVA fibre content is 0.2-0.3%. In addition, basalt fibres have a higher reinforcing effect on geopolymer mortars than PVA fibres at an early age. The reason can be the higher elastic modulus of basalt fibres, which benefits the stress dispersion and withstands part of the stress.

3.3. Drying Shrinkage of Geopolymer Mortars. Figure 4 shows the influence of the content of basalt fibres and PVA fibres on the drying shrinkage of geopolymer mortars. The shrinkage can be attributed to the internal water that evaporates from the pore network of the binder to the external environment at a relatively low level of humidity. Capillary stresses from the evaporation of capillary water during the drying process result in shrinkage strain. Most of the drying shrinkage occurs on the first day because of the rapid loss of internal water from freshly formed surfaces.

Figure 4(a) shows that the drying shrinkage of geopolymer mortars reinforced by basalt fibre experiences two stages. The drying shrinkage geopolymers rapidly increase at the initial stage and subsequently level off. The drying shrinkage first increases and subsequently decreases with increasing fibre content. The drying shrinkage was minimal when the basalt fibre content was 0.4% at 56 d. The 14-d drying shrinkage was 410×10^{-5} for the control group, which accounts for 92.5% of the 56-d drying shrinkage. For geopolymer mortars prepared with 0.4% basalt fibres, the 56-d drying shrinkage was 361×10^{-5} for mortars reinforced with 0.4% basalt fibres, which is a decrease of 18.5% compared to the control group. The high elastic modulus of basalt fibres increases the tensile strength of composites at the initial stage of plasticity and hardening and resists the deformation of matrices due to dehydration and drying. A proper content of basalt fibres can reduce the drying shrinkage and improve the volume stability of the material.

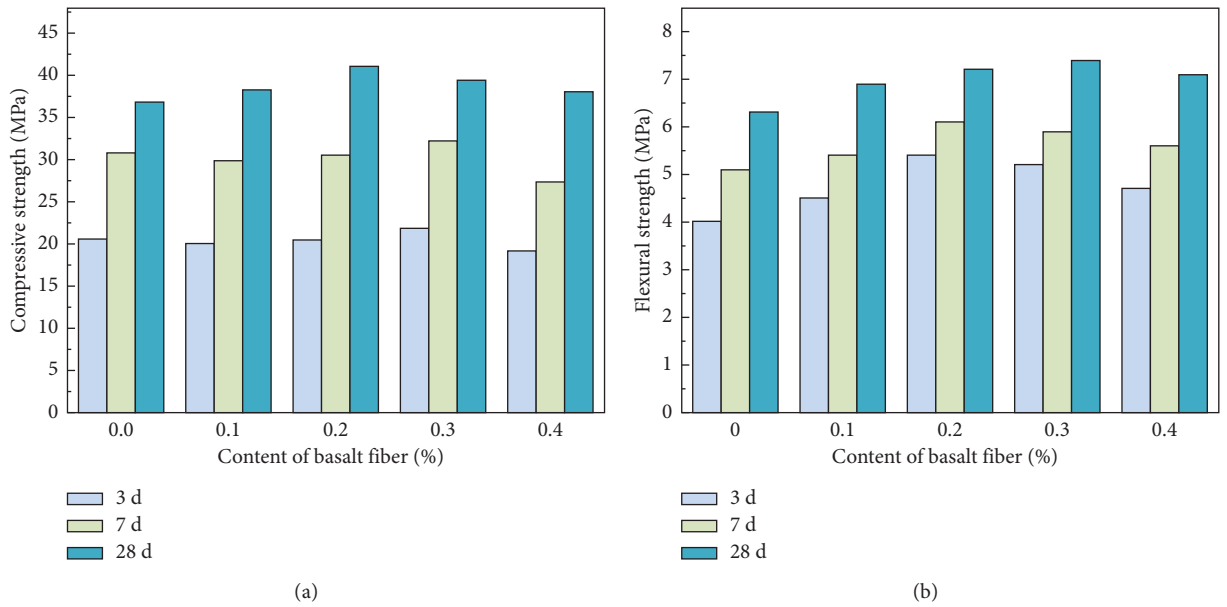

Figure 2: Strength of geopolymers mixed with different basalt fibre contents. (a) Compressive strength and (b) flexural strength.

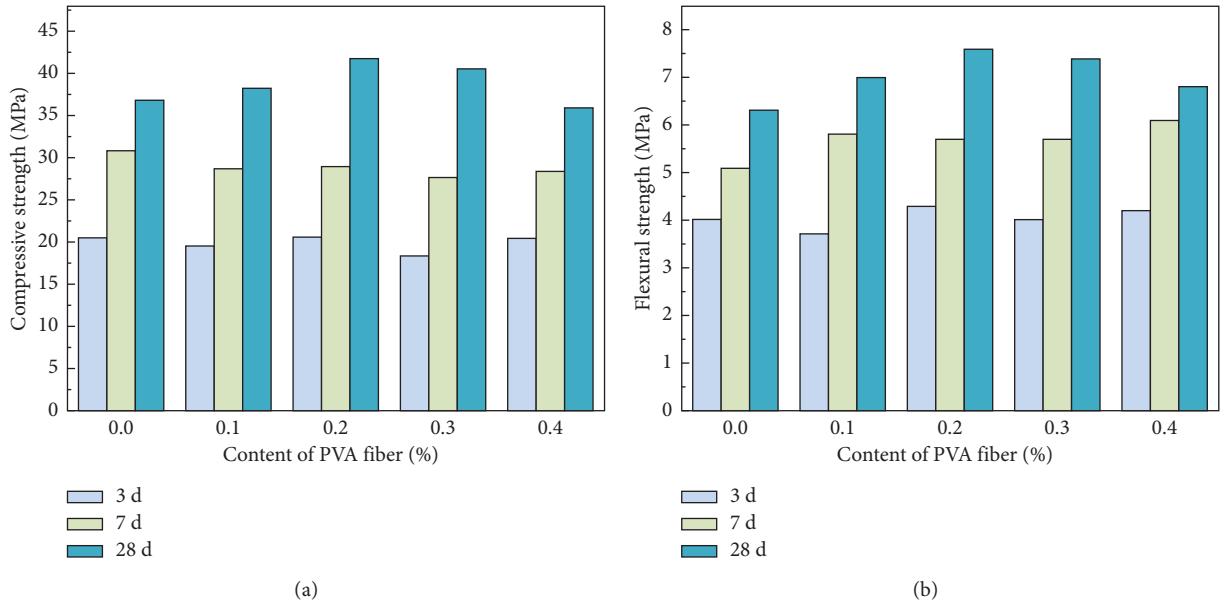

Figure 3: Strength of geopolymers with different PVA fibre contents. (a) Compressive strength and (b) flexural strength.

Figure 4(b) shows the influence of the PVA fibre content and drying age on the drying shrinkage of geopolymer mortars. The drying shrinkage of samples prepared with PVA fibres appeared to rapidly increase in the early stage and levelled off after 28 d of curing. A more obvious drying shrinkage appeared when the PVA fibre content was less than 0.3% compared to the control group. For example, the 56-d drying shrinkage of samples prepared at 0.2% volume fractions of PVA fibres was 540×10^{-5}, which is an increase of 21.9% compared to the control group. In contrast, the 56-d drying shrinkage was subject to an obvious limitation when the PVA fibre content increased to 0.4%, which is a decrease of 4% compared to the control group. Basalt fibres have a better effect on the drying shrinkage of geopolymer mortars than PVA fibres. The optimal content of fibres to inhibit drying shrinkage is different from that for the compressive strength. The 56-d drying shrinkage was maximal when 0.2% content of basalt fibres and PVA fibres was added, reaching 458×10^{-5} and 540×10^{-5}, respectively. Adding fibres with 0.4% volume fractions has the optimal reinforcing effect for drying shrinkage of geopolymer mortars. The fibres restrain the expansion and extension of the microcracks and disperse the stress caused by shrinkage, which reduces the shrinkage strain of the materials.

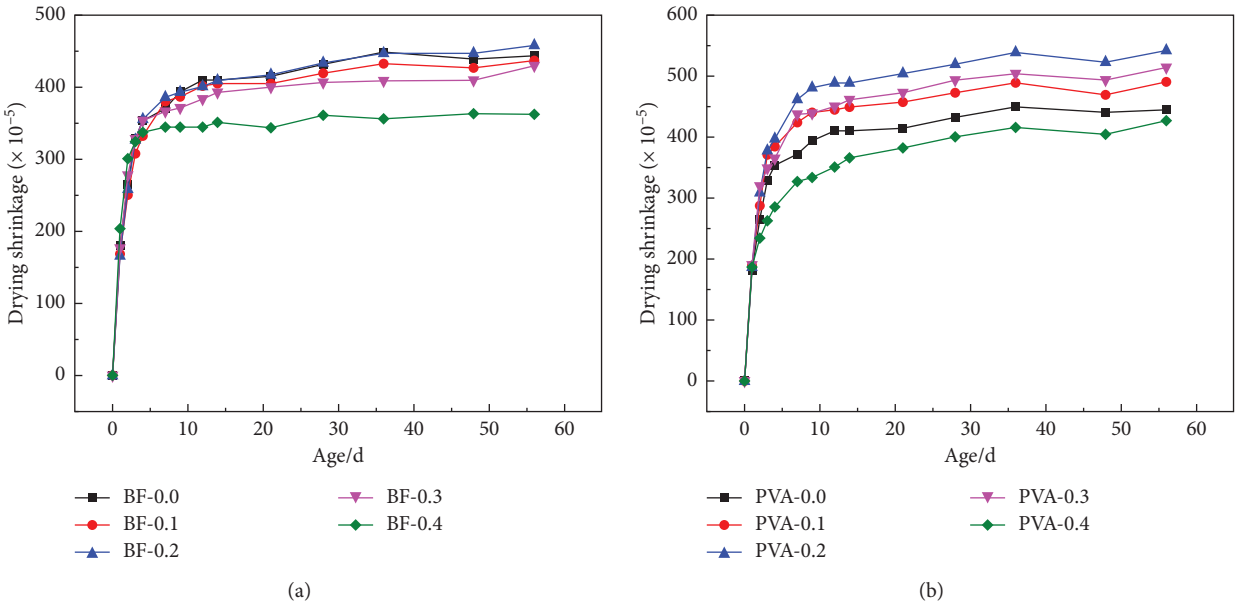

Figure 4: Effect of the content of (a) basalt fibre and (b) PVA fibre on drying shrinkage of geopolymer mortars.

Figure 5 shows the mass loss rate of geopolymer mortars in the drying process. Similar to the drying process, the mass loss rate of geopolymers increased with longer drying age. A more obvious mass loss occurred in the early stage. The relatively stable mass loss rate in the late stage is positively correlated with the drying shrinkage; that is, greater drying shrinkage corresponds to a greater water loss rate. Adding basalt fibres with appropriate content can effectively reduce the porosity of geopolymers and limit the internal water release from geopolymers. The geopolymer mortars have a lower early mass loss rate than the control group when the PVA fibre content is 0.4% but increases to become higher than that of the control group after 56 d of drying.

3.4. Autogenous Shrinkage of Geopolymer Mortars. Autogenous shrinkage of geopolymers derives from self-desiccation and chemical shrinkage, which reduces the volume. In this study, the autogenous shrinkage of geopolymers is measured after 24 h of moulding. Chemical shrinkage mainly occurs in the fresh state, so it will not be discussed in the following section. The autogenous shrinkage curves of the pastes evolve in two distinct stages: (1) the expansion behaviour during the initial curing age and (2) the shrinkage behaviour due to the further increase in shrinkage strain.

Figure 6(a) shows the influence of basalt fibres on the autogenous shrinkage of geopolymer mortars. The autogenous shrinkage increased with increasing setting age. The autogenous shrinkage of geopolymer mortars reinforced by the basalt fibres with 0.3% content was the minimum (278×10^{-5}) at 56 d, which decreases by 15.3% compared to the control group. The 14-d autogenous shrinkage reached 188×10^{-5} when the basalt fibre content was 0.4%, which accounted for 65.7% of the drying shrinkage at 56 d. Adding 0.3–0.4% volume fractions of basalt fibres has a relatively obvious inhibiting effect on autogenous shrinkage.

The influence of PVA fibres on the autogenous shrinkage of geopolymer mortars is different from the drying shrinkage, as shown in Figure 6(b). The autogenous shrinkage of geopolymer mortars decreased with increasing fibre content up to 0.3% volume fractions and subsequently increased. All contents of PVA fibres effectively reduced the autogenous shrinkage. The autogenous shrinkage of the geopolymer mortars increased with increasing setting age. Adding 0.3% content of PVA fibres mostly reduced the 56-d autogenous shrinkage. It reached 240×10^{-5} and decreased by 26.8% compared to the control group.

3.5. SEM Analysis. Figure 7 shows the SEM images of geopolymer mortars after 28 d of curing. Mass flocculent phases without regular shapes were found in all specimens. This is expected to be amorphous phases formed by the alkali-activated reaction and to form C–S–H gel and/or N-A-S-H [28, 29]. The alkali-activated reaction can generate C–S–H gels with smaller gel particles to fill the pore structure. Furthermore, gel phases can generate a three-dimensional network structure via a polymerization process [30, 31]. However, a few unreacted steel slag particles remain due to their low activity. Pores and cracks in geopolymer mortars can also be observed, as shown in Figure 7(a), which can be caused by shrinkage and water loss [32]. Single independent fibres can be observed and appear as a strong bond with the surrounding geopolymer mortar, which can effectively resist the crack extension and disperse the stress, as confirmed by Figure 7(b) [33]. Therefore, when the fibre content of both is 0.4%, the drying shrinkage is minimal. At this content, the fibres can effectively improve the mechanical properties and reduce drying shrinkage. However, comparing Figures *b* and *c*, PVA fibres will exhibit agglomeration phenomena due to better hydrophilicity, and there are microcracks at the combination surface of PVA fibres and ground poly. The gel and fibre fail to be closely

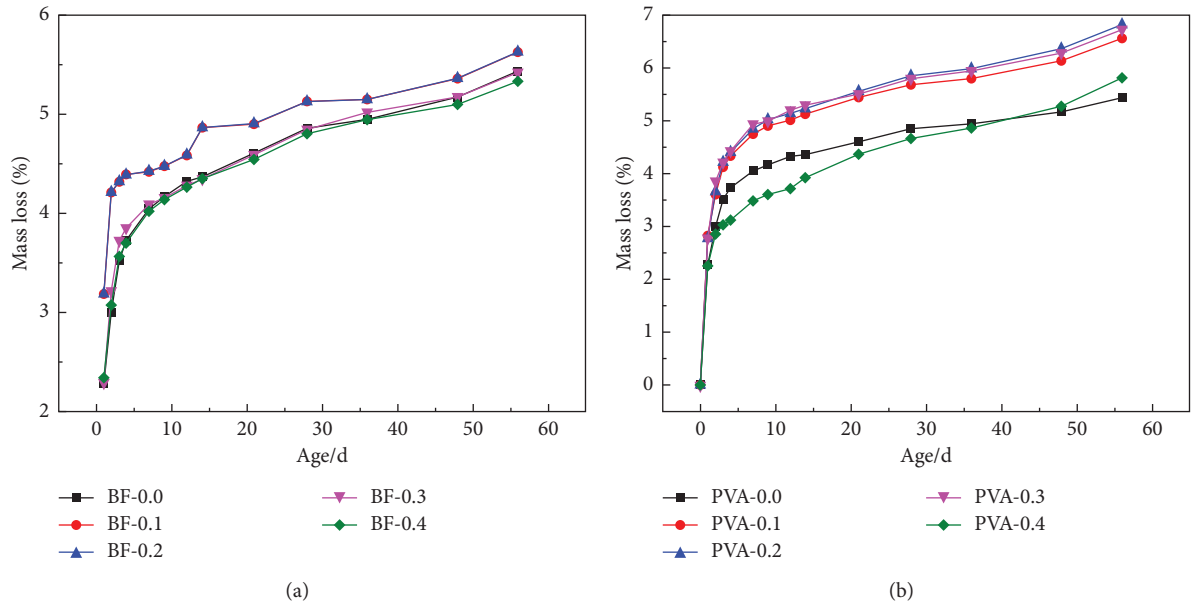

Figure 5: Effect of content of (a) basalt fibres and (b) PVA fibres on water loss rate of geopolymer mortars.

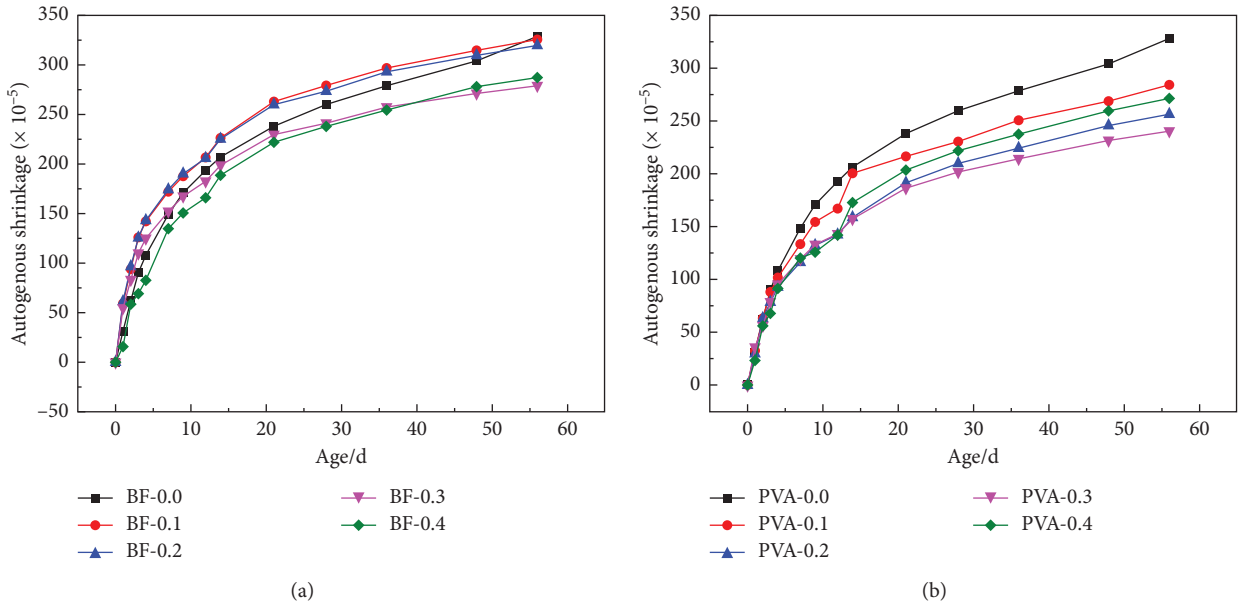

Figure 6: Effect of content of (a) basalt fibres and (b) PVA fibres on the autogenous shrinkage rate of geopolymer mortars.

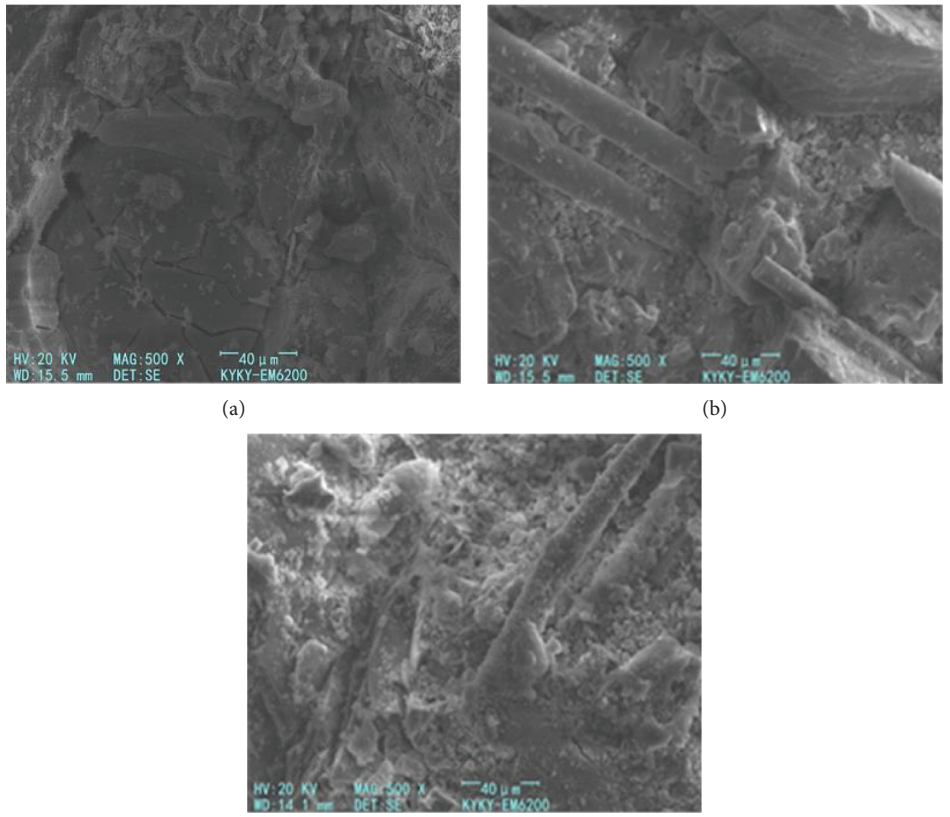

Figure 7: SEM images of geopolymer mortars to represent the dispersibility of fibres. (a) Blank sample. (b) Basalt fibres (0.4%. (c) PVA fibres (0.4%).

combined, the surrounding structure is looser, and more water is lost, so when PVA fibre doping is 0.4%, the drying shrinkage value is greater than that of basalt fibres.

4. Conclusions

In this article, the shrinkage and strength properties of geopolymer mortars made from blast furnace slag and steel slag reinforced by basalt fibre and polyvinyl alcohol (PVA) were studied. The main conclusions are as follows:

(1) After PVA fibres and basalt fibres have been added, the compressive strength and flexural strength of geopolymer mortars are improved. The flexural and compressive strengths first increase and subsequently decrease. The optimal content of basalt fibre and PVA fibre is 0.2–0.3%, and basalt fibre has a better toughening effect than PVA fibres.

(2) The drying shrinkage of geopolymer mortars first increases and subsequently decreases with increasing basalt fibre and PVA fibre contents. The mass loss rate shows the same trend as the drying shrinkage. The optimal content of basalt fibres and PVA fibres to limit drying shrinkage is 0.4%. PVA fibres will increase shrinkage due to their hydrophilicity compared to basalt fibres.

(3) The autogenous shrinkage test shows that when the content of both fibres is 0.3%, the self-shrinkage is minimal. SEM testing shows that the addition of fibres can effectively alleviate the stress concentration of geopolymer mortars and prevent crack propagation. However, excessive fibres can agglomerate, which results in a loss of strength.

Data Availability

The data used to support the findings of this study are included within the article.

Conflicts of Interest

The authors declare that they have no conflicts of interest.

Acknowledgments

This work was financially supported by the Project of Science and Technology of Henan Transportation Department (Grant no. 2018J4).

References

[1] G. Liang, H. Zhu, H. Li, T. Liu, and H. Guo, "Comparative study on the effects of rice husk ash and silica fume on the freezing resistance of metakaolin-based geopolymer,"

Construction and Building Materials, vol. 293, Article ID 123486, 2021.

[2] W. Long, J. Peng, Y. Gu, and J. Li, "Recycled use of municipal solid waste incinerator fly ash and ferronickel slag for eco-friendly mortar through geopolymer technology," *Journal of Cleaner Production*, vol. 307, Article ID 127281, 2021.

[3] K. Sedić, N. Ukrainczyk, V. Mandić, and N. Gaurina Međimurec, J. Šipušić, Carbonation of Portland-Zeolite and geopolymer well-cement composites under geologic CO_2 sequestration conditions," *Cement and Concrete Composites*, vol. 111, Article ID 103615, 2020.

[4] P. Zhang, Y. Zheng, K. Wang, and J. Zhang, "A review on properties of fresh and hardened geopolymer mortar," *Composites Part B: Engineering*, vol. 152, pp. 79–95, 2018.

[5] C. Suksiripattanapong, S. Horpibulsuk, P. Chanprasert, P. Sukmak, and A. Arulrajah, "Compressive strength development in fly ash geopolymer masonry units manufactured from water treatment sludge," *Construction and Building Materials*, vol. 82, pp. 20–30, 2015.

[6] S. S. Hossain, P. K. Roy, and C.-J. Bae, "Utilization of waste rice husk ash for sustainable geopolymer: a review," *Construction and Building Materials*, vol. 310, Article ID 125218, 2021.

[7] A. I. I. Helmy, "Intermittent curing of fly ash geopolymer mortar," *Construction and Building Materials*, vol. 110, pp. 54–64, 2016.

[8] C. D. Atiş, O. E. B. Görür, and C. Karahan, "Very high strength (120MPa) class F fly ash geopolymer mortar activated at different NaOH amount, heat curing temperature and heat curing duration," *Construction and Building Materials*, vol. 96, pp. 673–678, 2015.

[9] S. İlkentapar, C. D. Atiş, O. Karahan, and E. G. Avşaroğlu, "Influence of duration of heat curing and extra rest period after heat curing on the strength and transport characteristic of alkali activated class F fly ash geopolymer mortar," *Construction and Building Materials*, vol. 151, pp. 363–369, 2017.

[10] T. Yang, H. Zhu, and Z. Zhang, "Influence of fly ash on the pore structure and shrinkage characteristics of metakaolin-based geopolymer pastes and mortars," *Construction and Building Materials*, vol. 153, pp. 284–293, 2017.

[11] H. E. Elyamany, A. E. M. Abd Elmoaty, and A. M. Elshaboury, "Setting time and 7-day strength of geopolymer mortar with various binders," *Construction and Building Materials*, vol. 187, pp. 974–983, 2018.

[12] K. Chen, D. Wu, M. Yi, Q. Cai, and Z. Zhang, "Mechanical and durability properties of metakaolin blended with slag geopolymer mortars used for pavement repair," *Construction and Building Materials*, vol. 281, Article ID 122566, 2021.

[13] P. Zhang, K. Wang, J. Wang, J. Guo, and Y. Ling, "Macroscopic and microscopic analyses on mechanical performance of metakaolin/fly ash based geopolymer mortar," *Journal of Cleaner Production*, vol. 294, Article ID 126193, 2021.

[14] M. A. Malik, M. Sarkar, S. Xu, and Q. Li, "Effect of PVA/SiO2 NPs additive on the structural, durability, and fire resistance properties of geopolymers," *Applied Sciences*, vol. 9, no. 9, p. 1953, 2019.

[15] X. Guo and X. Pan, "Mechanical properties and mechanisms of fiber reinforced fly ash-steel slag based geopolymer mortar," *Construction and Building Materials*, vol. 179, pp. 633–641, 2018.

[16] W. Punurai, W. Kroehong, A. Saptamongkol, and P. Chindaprasirt, "Mechanical properties, microstructure and drying shrinkage of hybrid fly ash-basalt fiber geopolymer paste," *Construction and Building Materials*, vol. 186, pp. 62–70, 2018.

[17] R. Si, Q. L. Dai, S. C. Guo, and J. Wang, "Mechanical property, nanopore structure and drying shrinkage of metakaolin-based geopolymer with waste glass powder," *Journal of Cleaner Production*, vol. 242, Article ID 118502, 2019.

[18] I. Khan, T. Xu, A. Castel, R. I. Gilbert, and M. Babaee, "Risk of early age cracking in geopolymer concrete due to restrained shrinkage," *Construction and Building Materials*, vol. 229, Article ID 116840, 2019.

[19] D. S. Perera, O. Uchida, E. R. Vance, and K. S. Finnie, "Influence of curing schedule on the integrity of geopolymers," *Journal of Materials Science*, vol. 42, no. 9, pp. 3099–3106, 2007.

[20] R. J. Thomas, D. Lezama, and S. Peethamparan, "On drying shrinkage in alkali-activated concrete: improving dimensional stability by aging or heat-curing," *Cement and Concrete Research*, vol. 91, pp. 13–23, 2017.

[21] Y. Ling, K. Wang, and C. Fu, "Shrinkage behavior of fly ash based geopolymer pastes with and without shrinkage reducing admixture," *Cement and Concrete Composites*, vol. 98, pp. 74–82, 2019.

[22] P. Kamhangrittirong, P. Suwanvitaya, W. Witayakul, P. Suwanvitaya, and P. Chindaprasirt, "Factors influence on shrinkage of high calcium fly ash geopolymer paste," *Advanced Materials Research*, vol. 610, pp. 2275–2281, 2013.

[23] K. Mermerdaş, Z. Algin, and Ş Ekmen, "Experimental assessment and optimization of mix parameters of fly ash-based lightweight geopolymer mortar with respect to shrinkage and strength," *Journal of Building Engineering*, vol. 31, Article ID 101351, 2020.

[24] C. Ridtirud, P. Chindaprasirt, and K. Pimraksa, "Factors affecting the shrinkage of fly ash geopolymers," *International Journal of Minerals, Metallurgy, and Materials*, vol. 18, no. 1, pp. 100–104, 2011.

[25] P. Duan, C. Yan, W. Luo, and W. Zhou, "Effects of adding nano-TiO 2 on compressive strength, drying shrinkage, carbonation and microstructure of fluidized bed fly ash based geopolymer paste," *Construction and Building Materials*, vol. 106, pp. 115–125, 2016.

[26] A. Saloni, A. Parveen, and M. Thong, "Enhanced properties of high-silica rice husk ash-based geopolymer paste by incorporating basalt fibers," *Construction and Building Materials*, vol. 245, Article ID 118422, 2019.

[27] A. Noushini, M. Hastings, A. Castel, and F. Aslani, "Mechanical and flexural performance of synthetic fibre reinforced geopolymer concrete," *Construction and Building Materials*, vol. 186, pp. 454–475, 2018.

[28] Z. Xu, J. Yue, G. Pang, R. Li, P. Zhang, and S. Xu, "Influence of the activator concentration and solid/liquid ratio on the strength and shrinkage characteristics of alkali-activated slag geopolymer pastes," *Advances in Civil Engineering*, vol. 2021, Article ID 6631316, 11 pages, 2021.

[29] J. Xu, A. Kang, Z. Wu, P. Xiao, and Y. Gong, "Effect of high-calcium basalt fiber on the workability, mechanical properties and microstructure of slag-fly ash geopolymer grouting material," *Construction and Building Materials*, vol. 302, Article ID 124089, 2021.

[30] S. Saxena and A. R. Tembhurkar, "Developing biotechnological technique for reuse of wastewater and steel slag in bioconcrete," *Journal of Cleaner Production*, vol. 229, pp. 193–202, 2019.

[31] X. Guo and G. Xiong, "Resistance of fiber-reinforced fly ash-steel slag based geopolymer mortar to sulfate attack and

drying-wetting cycles," *Construction and Building Materials*, vol. 269, Article ID 121326, 2021.

[32] C. Seneviratne, C. Gunasekara, D. Law, S. Setunge, and D. Robert, "Creep, shrinkage and permeation characteristics of geopolymer aggregate concrete: long-term performance," *Archives of Civil and Mechanical Engineering*, vol. 20, no. 4, pp. 1–15, 2020.

[33] S. Samal and I. Blanco, "An application review of fiber-reinforced geopolymer composite," *Fibers*, vol. 9, no. 4, p. 23, 2021.